Proceeding to the LHC seminar talk *Update of the* $B^0 \rightarrow K^{*0}\ \mu^+\ \mu^-$ *angular analysis at LHCb experiment* held by Eluned Smith on behalf of the LHC collaboration on 13th of March 2020.

Nils Breer

Technische Universität Dortmund

The LHCb collaboration has published new results regarding flavor changing neutral currents based on recent studies for physics beyond standard model. FCNC are very promising decay types since they only occur at loop level and are therefore very sensitive for new physics. The data from the previous analysis in 2011 and 2012 were expanded by the 2016 data which results in twice the amount of statistics. With this and a deeper understanding of theoretical uncertainties an angular analysis was performed. The hints on a local tension in $P_5{}'$ were confirmed with this analysis. One of the explanations points to a shift in the wilson coefficient C_9. The most sensitive observables to C_9 are the q^2 dependence of the forward-backward asymmetry and $P_5{}'$. The significance of the tension results in 2.7 - 3.3σ. The complete set of measurements into the $b \rightarrow s\mu^-\mu^+$ transition performed by various experiments includes the observables R_K and R_K^*, describing ratios corresponding to $B \rightarrow K^*ll$ decays involving muons and electrons. This analysis focusses on observables in the P_i and S_i basis and does not include R_K and R_K^*.

The stated Process is of such importance because the $b \rightarrow s\mu\mu$ transition is forbidden at tree level due to FCNC and can only occur at loop order. Because of that, these processes are much more sensitive to new physics(NP).

To gather information about short distance NP above the SM energy scale μ, wilson coefficients $C_i(\mu)$ and low-energy QCD Operators O_i are used to describe that.

The wilson coefficients C_7, C_9 and C_{10} are of great importance since observables like the forward-backward asymmetry and $P_5{}'$ are sensitive for C_9 especially.

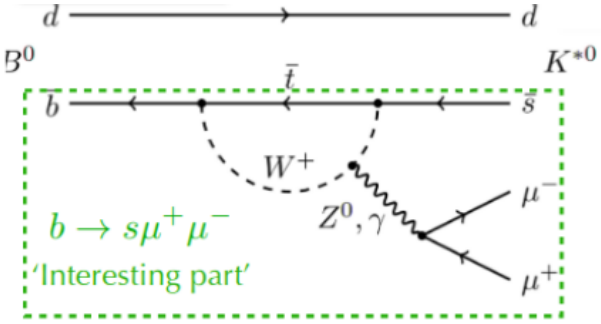

Figure 1: The SM process of $b \rightarrow s\mu^-\mu^+$. The green box can be described with NP models.

In an effective theory, C_9 and C_{10} are used to describe the contribution from loops, in which electroweak gauge bosons are produced. wilson coefficient C_7 describes the contribution from loopdiagramms which produce photons from the loops.

This can be summarized by an effective hamiltonian

$$H_{eff} = -\frac{4G_f}{\sqrt{2}} \mathrm{V}_{tb}\mathrm{V}_{ts}^* \sum_i C_i \cdot O_i + \mathrm{h.c.}$$

G_F is Fermi's constant, μ ist the renormalization scale, $\mathrm{V}_{tb}\mathrm{V}_t s^*$ is the contains leading flavor factors of the SM which lie in the CKM matrix elements V_{ij}

To measure the decay rate as a function of angles of the decay products, an angular analysis is performed. This is motivated by the fact, that the K^{0*} is a meson with spin 1 therefore three polarisation states. This results in a rich angular structure. The definition of the angular observables θ_k, θ_l and ϕ is schematically shown in figure 2

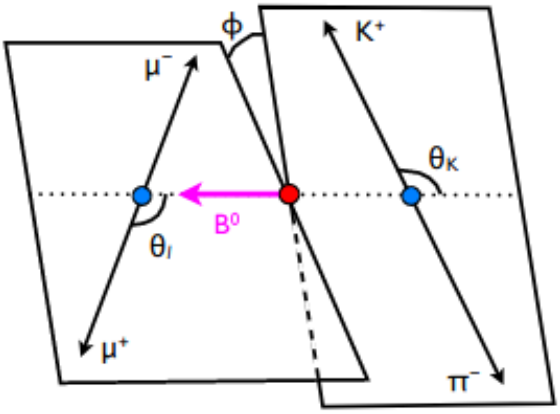

Figure 2: image of the angular observables.[4]

In this analysis, the forward-backard asymmetry A_{FB}, F_L the fraction of the longitudinal polarisation of the K^{*0} and the decay rate of the process $B^0 \to K^{*0}\mu\mu$ was measured. The definition of the angular observables are the following. θ_l is the angle between the negatively charged lepton and $\bar{B}$ in the dimuon center of mass system (c.m.s). θ_k is the angle between the Kaon and the $\bar{B}$ in the K^{*0} c.m.s.. The angle between the K^{*0}-plane and the dimuon-plane is defined by the angle ϕ[3].
Considering that S-wave contribution, spinless $K^+\pi^-$ constellations, can pollute the measurement, therfore a parametrization such as $(1 - F_S)$ for this was taken into account where $(1 - F_S)$ is the S-wave fraction which describes the amount of S-wave contribution. The interference Amplitude between P-wave and S-wave decays are parametrized by A_S. The angular distribution[4] for the $B^0 \to K^{*0}\mu\mu$ decay reads

$$\frac{1}{\Gamma}\frac{\mathrm{d}^3\Gamma}{\mathrm{d}\theta_k \mathrm{d}\theta_l \mathrm{d}q^2} = \frac{9}{16} f(F_S, A_S, \theta_k, \theta_l, A_{FB}, F_L) \tag{1}$$

Since A_{FB}, F_L and $\mathcal{A} \times E$ do not depend on the angle ϕ, it is already integrated out. The angular description for The B and $\bar{B}$ are combined afterwards and expanded into a sum of the angular variables multiplied with a fitparameter, which are the A_{FB}, F_L and S_i, as seen in figure 3, which are called CP-averaged observables. The CP asymmetries need to be analyzed further because NP could contribute differently to CP-conjugated processes.
Then the fit in the S_i basis was reparametrised to the P_i basis. This was done to eliminate first

$$\left.\frac{1}{\mathrm{d}(\Gamma+\bar{\Gamma})/\mathrm{d}q^2}\frac{\mathrm{d}(\Gamma+\bar{\Gamma})}{\mathrm{d}\cos\theta_l\,\mathrm{d}\cos\theta_K\,\mathrm{d}\phi}\right|_{\mathrm{P}} = \frac{9}{32\pi}\Big[\tfrac{3}{4}(1-F_L)\sin^2\theta_K + F_L\cos^2\theta_K + \tfrac{1}{4}(1-F_L)\sin^2\theta_K\cos 2\theta_l - F_L\cos^2\theta_K\cos 2\theta_l + S_3\sin^2\theta_K\sin^2\theta_l\cos 2\phi + S_4\sin 2\theta_K\sin 2\theta_l\cos\phi + S_5\sin 2\theta_K\sin\theta_l\cos\phi + \tfrac{4}{3}A_{FB}\sin^2\theta_K\cos\theta_l + S_7\sin 2\theta_K\sin\theta_l\sin\phi + S_8\sin 2\theta_K\sin 2\theta_l\sin\phi + S_9\sin^2\theta_K\sin^2\theta_l\sin 2\phi\Big].$$

F_L :fraction of longitudinal polarisation of the K^{*0}

A_{FB} :forward-backward asymmetry of dimuon system

Figure 3: Angular description for B and $\bar{B}$ combined.

order uncertainties in the form factors primarily. The fit to the angular distribution yields seven CP violating observables including F_L.

$$P_1 = \frac{2S_3}{1-F_L} \qquad P_{4,5,8}{}' = \frac{S_{4,5,8}}{\sqrt{F_L\,(1-F_L)}}$$
$$P_2 = \frac{2}{3}\frac{A_{FB}}{1-F_L} \qquad P_6{}' = \frac{S_7}{\sqrt{F_L\,(1-F_L)}}$$
$$P_3 = \frac{-S_9}{1-F_L}$$

The angular distribution can be reduced to

$$\frac{1}{\Gamma}\frac{\mathrm{d}^3\Gamma[\bar{B}^0 \to \bar{K}^{0*}\mu^+\mu^-]}{\mathrm{d}\cos\theta_l \mathrm{d}\cos\theta_k \mathrm{d}q^2} = \frac{9}{16}\sum_i S_i(q^2_{min}, q^2_{max}) f_i(\vec{\Omega})$$

in the S_i basis where $\vec{\Omega} = (\cos\theta_l, \cos\theta_k)$. The S_i basis contains the six angular coefficients which are the combinations of the K^{0*} amplitudes. These amplitudes describe the polarization states of the Kaon.
This analysis especially focuses heavily on the tension induced by $P_5{}'$, since it is a very sensitive variable for C_9. This can be seen in the range of 4 - 8 $\frac{\mathrm{GeV}^2}{c^4}$ displayed in figure 4. The discrepancy is 2.8σ for the q^2 intervall from 4 - 6 $\frac{\mathrm{GeV}^2}{c^4}$ and 3σ for the 6 - 8 $\frac{\mathrm{GeV}^2}{c^4}$ intervall. For every collaboration a discrepancy between the SM and the measurement is visible, but the CMS measurement is the closest the the SM prediction.
For this analysis the data sets used are from the years 2011, 2012 and 2016. The data sets from 2011 and 2012 are from run 1. The 2011 data was taken at a centre of mass energy of $\sqrt{s} = 7\,\mathrm{TeV}$, the 2012 data at $\sqrt{s} = 8\,\mathrm{TeV}$ and the added data set from 2016 was taken at $\sqrt{s} = 13\,\mathrm{TeV}$. Adding the 2016 data also doubled the statistic to around 4,7/fb.
For the selection of candidates it is required, that the impact paramters for the daughter par-

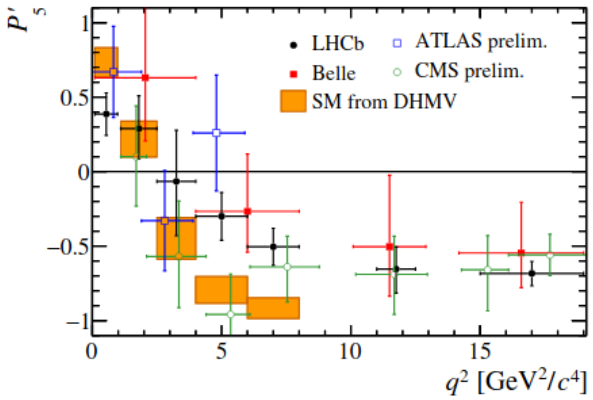

Figure 4: tension in P_5'.[2]

ticles are quite significant since they do not originate from the primary vertex. Daughter particles that come from the primary vertex need to have a very small impact parameter and also a quality vertex is necessary. That means the track fit $\frac{\chi^2}{dof}$ must be small, where dof are the degrees of freedom. Also two muon candidates, a kaon and a pion are required. To suppress peaking background as seen in figure 5 the particle identification is used. The FCNC process here is described by $B^0 \to K^{0*}\mu\mu$, but the subprocesses such as $B^0 \to K^{0*}\,(\bar{c}c \to \gamma^* \to \mu\mu)$ are statistical relevant since they proceed at tree level. Therefore charmonium resonances pollute the q^2 spectrum, especially at the J/$\Psi(1S)$ and the $\Psi(2S)$ mass. Around these peaks a mass-veto region is defined where signal decays are neglected if they fall into the veto region. Left, in between and on the right of the peaks the signal regions are defined. A multivariate analysis(MVA)[6] is performed to suppress combinatorial background, incorrectly vertexed tracks, even further. MVA is a machine learning technique in which a classifier or regressor takes several features to learn from and to make a prediction on what is background and what belongs to the signal. To suppress $J/\Psi \to ll$ contributions, the invariant mass spectrum is looked at. The most common features are: small momentum particles and small opening angles and a large dE/dx. Other input variables are the B^0 decay time, vertex-fit quality, momentum and transverse momentum of B^0 candidate, θ_{DIRA} as well as particle identification from the RICH detector. θ_{DIRA} describes the opening angle between the reconstructed B^0 momentum and the vector connecting the reconstructed B^0 decay vertex to the primary vertex. The classifier is trained on $B \to J/\Psi K^{0*}$ candidates as signal. The background consists of candidates from the mass region $m(B \to K^+\pi^-\mu^+\mu^-) \in [5350\mathrm{MeV}, 7000\mathrm{MeV}]$. Since the detector cannot know which lepton pairs belong together, all possible combinations are tested. Combinations with same signed leptons (N^{++} or N^{--}) are always uncorrelated so the signal S results in $S = N^{+-} - (N^{++} + N^{--})$. This is called the like-sign method[5]. N^{+-} are the opposite sign lepton pairs.

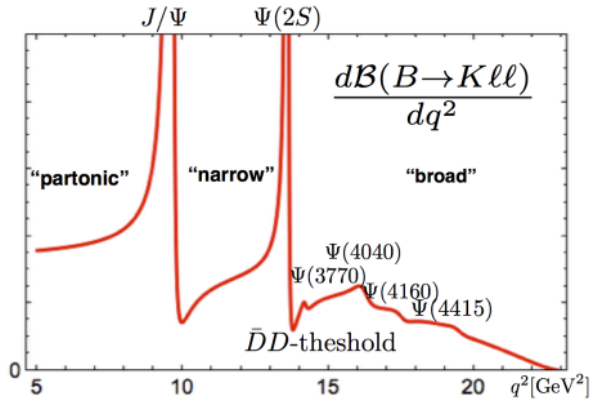

Figure 5: spectrum in q^2 for the lepton pair in Kll branching fraction[2].

For the full fit model the shape of the invariant mass plots are used to determine the amount of signal and background in the data.

$$\mathrm{PDF}_{total} = f_{sig}\mathrm{PDF}_{sig}(\vec{\Omega}, m) + (1 - f_{sig})\mathrm{PDF}_{bkg}(\vec{\Omega}, m)$$

The PDF function can be separated into an angular part and a massive part. After that a maximum likelihood fit is performed. As seen in figure 6 the massive part of the signal PDF is a gaussian function with a radiative tail and the background PDF results in an exponential function.
Because of the factorization of the signal and background PDF

$$\mathrm{PDF}_{sig}(\vec{\Omega}, m) = \mathrm{PDF}_{sig}(\vec{\Omega}) \times \mathrm{PDF}_{sig}(m)$$
$$\mathrm{PDF}_{bkg}(\vec{\Omega}, m) = \mathrm{PDF}_{bkg}(\vec{\Omega}) \times \mathrm{PDF}_{bkg}(m)$$

the angular part of the signal PDF of the Run 1 data and the data from 2016 are shared

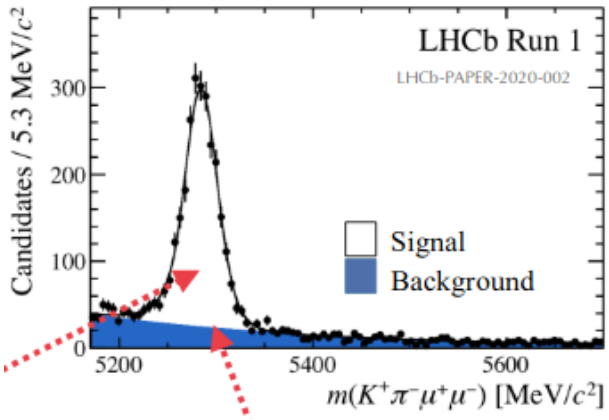

Figure 6: invariant B mass of Run 1 LHCb data.

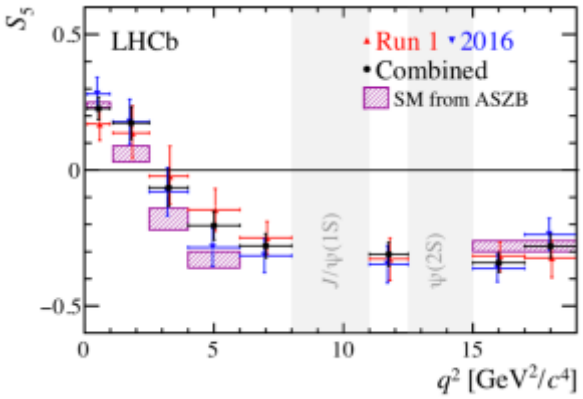

Figure 7: angular observable S_5 after the analysis.

in the analysis to perform a simultaneous fit $\sum_i S_{i,q^2_{bin}} f_i(\Omega)$. This is possible since they do not share the same mass and angular background because the conditions in the 2016 data sample differs from Run 1 data.

The efficiency needs correction since it's behavior is not flat. Legendre polynomials are used for the dimuon mass and the three angles which results in a 4D formular. The correlation between the observables negates the factorization of the 4D function to 1D functions.

The dominant systematic uncertainties are acceptance variations with q^2, peaking backgrounds and bias corrections as seen in figure 5. The uncertainty related to the contribution from the S-wave or P+S interference is evaluated by taking the difference between the default results, obtained by fitting with a function accounting for the S-wave (1), with the results from a fit performed with no S-wave or interference terms where $F_S = 0$ and $A_S = 0$.[4] Bias relates to the S-wave contribution F_S. If it is small, the angular spectrum is biased towards the P-wave. If $F_S \approx 1$, it is biased towards the S-wave.

Taking all that into account S_5 is in a quite good agreement with the SM and the Run 1 and 2016 measurement are very similar too.7 Also the local tension in P_5' is in a better agreement with the SM than before.8 With the datasets from Run 1 and 2016 combined a deviation from the SM of 2,5 in the $q^2 \in [4.0, 6.0] \frac{\text{GeV}^2}{c^4}$ bin was yielded. For the $q^2 \in [6.0, 8.0] \frac{\text{GeV}^2}{c^4}$ bin a deviation of 2,9 was yielded.

A shift in Re(C_9) clearly shows, that improvements in the overall significance can be made

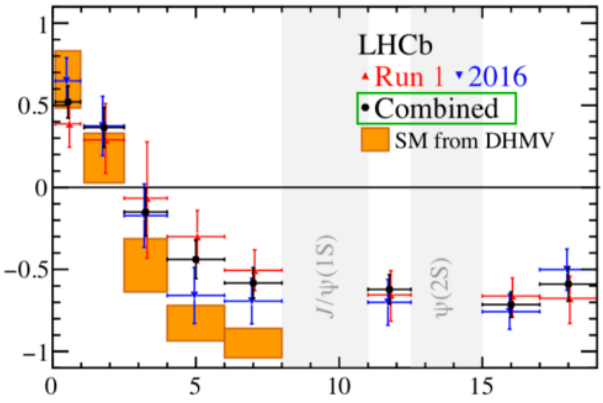

Figure 8: local tension in P_5' after the analysis.

as seen in figure 9. Figure 10 shows the angular observable P_5' as a function of q^2. Two variations of the wilson coefficient C_9 are displayed. These preferred variations close the gap between the SM prediction the data which would reduce local tension.

With that being said, the results presented in the seminar emphasize the overall tension proposed in Run 1 data from previous measurements. The higher overall tension does not confirm new physics but only hint at it. Different measurements at different scales could yield a deeper understanding an a more precise measurement which might confirm the hints. Futher studies in $b \to s$ transitions such as $b \to s\gamma$ could contribute to the analysis[1]. In order to study ne physics at higher scales, an angular analysis is important since the optimised basis reduce the theoretical uncertainties from form factors.

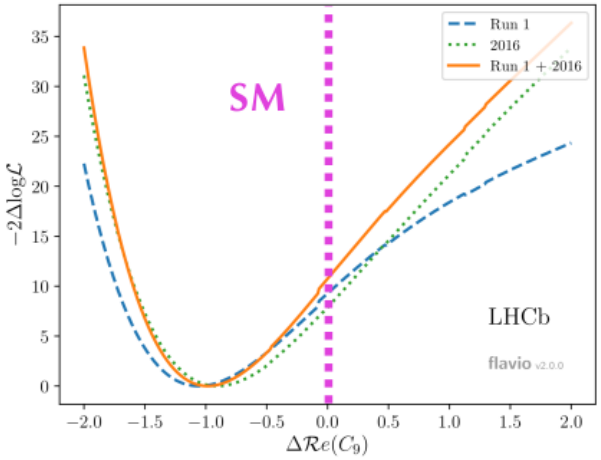

Figure 9: shift in the real part of C_9 yielded from the analysis.

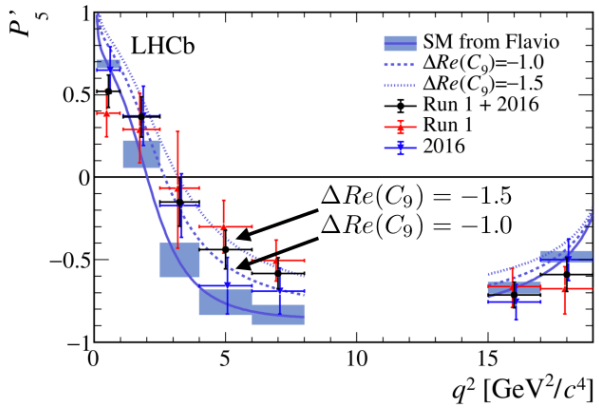

ıre 10: angular observable P_5' function of q^2. SM prediction theory with shifted C_9.

References

[1] Frederik Beaujean, Christoph Bobeth, and Danny van Dyk. "Comprehensive Bayesian analysis of rare (semi)leptonic and radiative B decays." In: *Eur. Phys. J. C* 74 (2014). [Erratum: Eur.Phys.J.C 74, 3179 (2014)], p. 2897. DOI: 10.1140/epjc/s10052-014-2897-0. arXiv: 1310.2478 [hep-ph].

[2] T. Blake et al. "Round table: Flavour anomalies in b → sl+l− processes." In: *EPJ Web Conf.* 137 (2017). Ed. by Y. Foka, N. Brambilla, and V. Kovalenko, p. 01001. DOI: 10.1051/epjconf/201713701001. arXiv: 1703.10005 [hep-ph].

[3] Christoph Bobeth, Gudrun Hiller, and Danny van Dyk. "The Benefits of $\bar{B}- > \bar{K}^* l^+ l^-$ Decays at Low Recoil." In: *JHEP* 07 (2010), p. 098. DOI: 10.1007/JHEP07(2010)098. arXiv: 1006.5013 [hep-ph].

[4] Serguei Chatrchyan et al. "Angular Analysis and Branching Fraction Measurement of the Decay $B^0 \to K^{*0}\mu^+\mu^-$." In: *Phys. Lett. B* 727 (2013), pp. 77–100. DOI: 10.1016/j.physletb.2013.10.017. arXiv: 1308.3409 [hep-ex].

[5] Bjørn Bäuchle Stefan Kniege. *How to subtract combinatorial Background*. URL: https://fias.frankfurtium.de/downloads/04_hqm_cb.pdf (visited on 08/09/2020).

[6] R. E. Schapire Y. Freund. *A Decision-Theoretic Generalization of On-Line Learning and an Application to Boosting*. URL: https://doi.org/10.1006/jcss.1997.1504 (visited on 08/14/2020).